Flexural behavior of side-by-side box-beam bridges: A comparative study

Nabil F. Grace, Kapil D. Patki, Eslam M. Soliman, and Joseph Q. Hanson

Editor's quick points

- Load-distribution and strain-distribution tests were conducted on two box-beam bridge models (one reinforced with prestressed carbon-fiber-composite cable [CFCC] and one reinforced with conventional prestressed steel strands) in their uncracked and cracked stages.
- The conventionally reinforced bridge model was under-reinforced to achieve ductility by yielding of the steel.
- The CFCC reinforced bridge model was over-reinforced to achieve ductility by crushing of the concrete to develop a plastic hinge mechanism.
- Both bridge models exhibited acceptable ductility in the form of deflections and cracking before failure.

Corrosion of steel reinforcement in side-by-side box-beam bridges is a common problem caused by longitudinal cracks in the deck slab over the shear-key area. Longitudinal cracks develop as a result of differential rotation between the adjacent box beams due to eccentric application of service loads.[1] The longitudinal cracks cause the bridge to lose its structural integrity. In addition, these longitudinal cracks conduct chloride ions from deicing salts to the steel reinforcement.[2] The chloride ions promote the corrosion of unprotected steel, eventually leading to cracking and spalling of the concrete in the surrounding areas. However, the application of transverse post-tensioning (TPT) forces, along with an adequate number of TPT diaphragms, can be used to control cracking in the longitudinal direction of the deck.[3] Alternatively, the level of TPT forces and the number of TPT diaphragms recommended by the Michigan Department of Transportation (MDOT) *Prestressed Concrete Box-Beam and Post-Tensioning Details*[4] are not adequate to eliminate the longitudinal cracks in the deck slab over the shear-key joints.[5]

In addition to TPT, the use of carbon-fiber-composite cable (CFCC) as reinforcement provides an alternative means of eliminating deterioration of concrete structures due to corrosion of steel reinforcement.[6] In addition to its noncorrosive characteristics, CFCC reinforcement has advantages such as light weight, high fatigue endurance, and high longitudinal tensile strength.[7] Hence, the use of fibrous composite materials is now considered the best solution to the corrosion problem associated with conventional steel reinforcement, thereby reducing the maintenance cost of the structures considerably.[8] The use of unbonded carbon-fiber-reinforced polymer (CFRP) strands for TPT has successfully been implemented in the

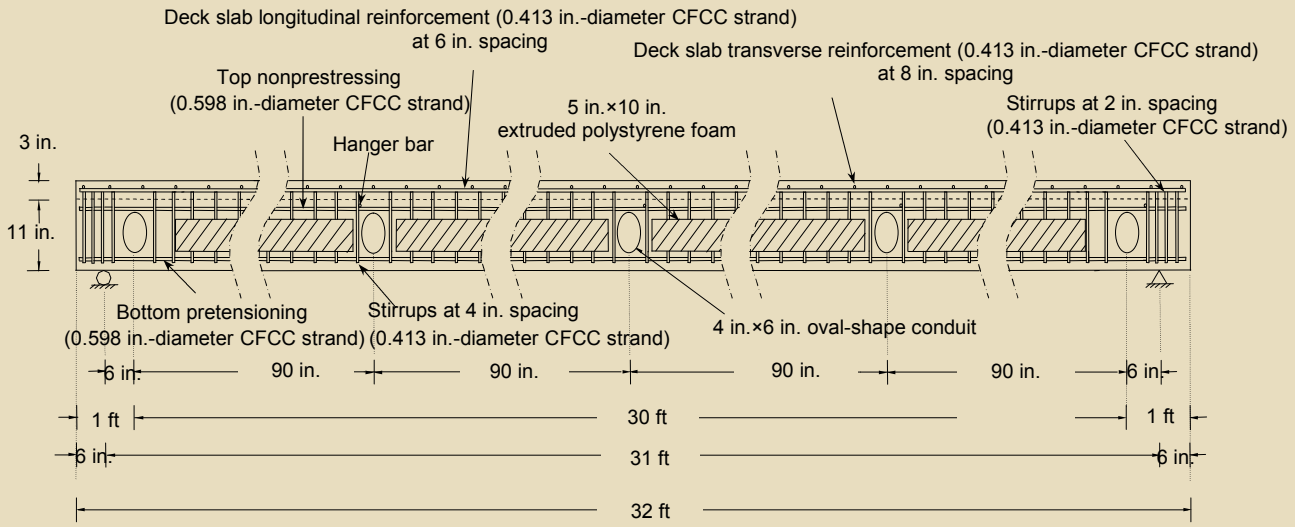

Figure 1. Longitudinal cross-sectional details of CFCC bridge model. Note: CFCC = carbon-fiber-composite cable. 1 in. = 25.4 mm; 1 ft = 0.305 mm.

field, for example, in the construction of the Bridge Street Bridge in Southfield, Mich., the first three-span CFRP prestressed concrete highway bridge in the United States.[9]

Two precast, prestressed concrete box-beam bridge models reinforced with CFCC and conventional steel strands were constructed, instrumented, and tested. The conventionally reinforced bridge model was designed to be under-reinforced in accordance with the AASHTO design philosophy espoused by MDOT[4] to provide ductility by yielding of the steel. The CFCC-reinforced bridge model was designed to be over-reinforced in accordance with ACI 440,[7] achieving ductility by crushing the concrete and developing a plastic hinge mechanism. The purpose of this investigation was to compare qualitatively the flexural behavior of the two bridge models in terms of the load-deflection response, load-strain response, ultimate strength, failure mode, response of unbonded TPT CFCC strands, and energy ratios.

Experimental investigation

Two 30-deg-skew, half-scale bridge models, each consisting of four box beams with different reinforcement, were constructed. Both bridge models were identical with respect to their cross section and longitudinal section. The clear spans of both bridge models were 31 ft (9.5 m), with a 3-in.-thick (75 mm) reinforced deck slab placed on the box beams. Each box beam was 18 in. (460 mm) wide and 11 in. (280 mm) deep. In accordance with MDOT design specifications,[4] the box beams were provided with five transverse diaphragms spaced equally at 7.5 ft (2.3 m) to facilitate TPT. Each diaphragm in both bridge models was provided with two unbonded TPT CFCC strands. **Figures 1** through **4** show the longitudinal and cross-sectional details of both bridge models.

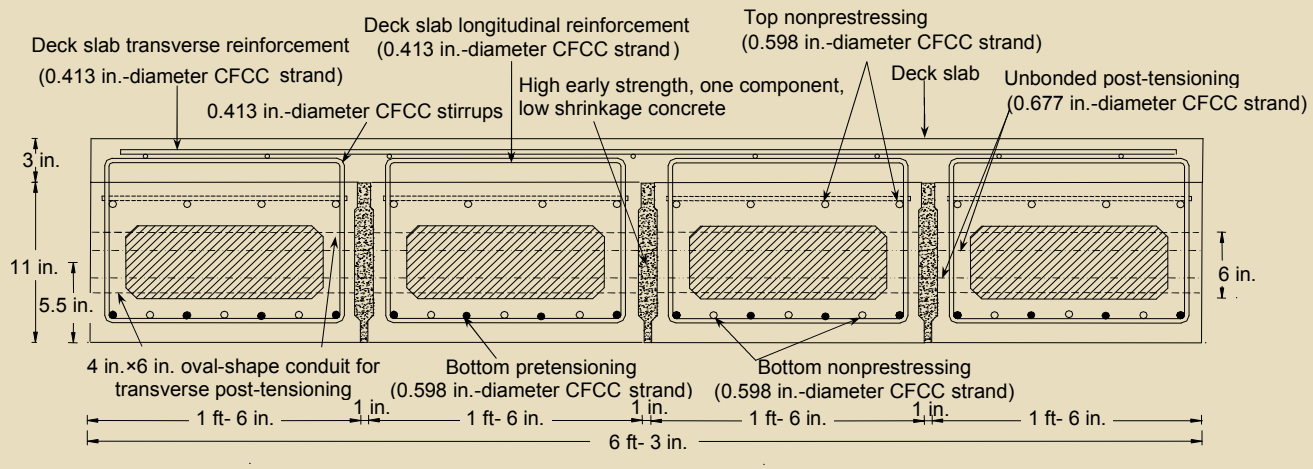

Figure 2. Cross-sectional details of CFCC bridge model. Note: CFCC = carbon-fiber-composite cable. 1 in. = 25.4 mm; 1 ft = 0.305 m.

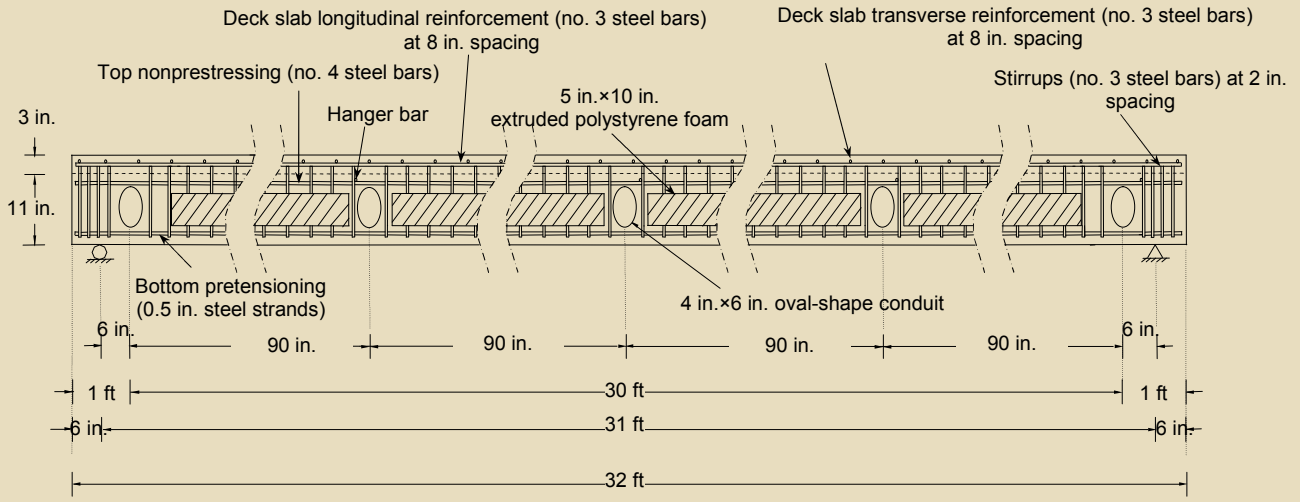

Figure 3. Longitudinal cross-sectional details of conventional bridge model. Note: no. 3 = 10M; no. 4 = 13M; 1 in. = 25.4 mm; 1 ft = 0.305 m.

Construction details of the box beams

Two separate sets of formwork were made for each interior and exterior box beam. The flexural reinforcement for the box beams comprised both prestressed and nonprestressed cables. Each box beam in the CFCC bridge model had four 0.6-in.-diameter (15 mm) prestressed CFCCs made of seven primary strands. In addition, seven 0.6-in.-diameter (15 mm) nonprestressed CFCCs made of seven primary strands were provided on top and bottom. The stirrups were 0.4-in.-diameter (10 mm) CFCC and protruded 1.1 in. (28 mm) from the top surface of the box beam to promote composite action and develop monolithic behavior at the connection with the deck slab.

The steel cages for the conventional bridge model consisted of four no. 4 (13M) deformed mild steel reinforcing bars at the top and bottom. In addition, three 0.5-in.-diameter (13 mm) seven-wire steel strands were provided as prestressing strands. The stirrups protruded 1.1 in. (28 mm) from the top surface of the box beams.

To create a hollow portion within the box beam, 5 in. (130 mm) × 10 in. (250 mm) extruded polystyrene foam was provided in both bridge models and covered the entire length between the two diaphragms. A 6 in. (150 mm) × 4 in. (100 mm) oval-shaped, galvanized steel tube was inserted to provide a duct for the unbonded TPT CFCCs.

In the CFCC bridge model, an average prestressing force of 25 kip (110 kN) was applied to each pretensioned CFCC, thus constituting a 100 kip (445-kN) prestressing force per beam. In the conventional bridge model, the two exterior box beams were prestressed with an average force of 20 kip (89 kN) per strand and the two interior box

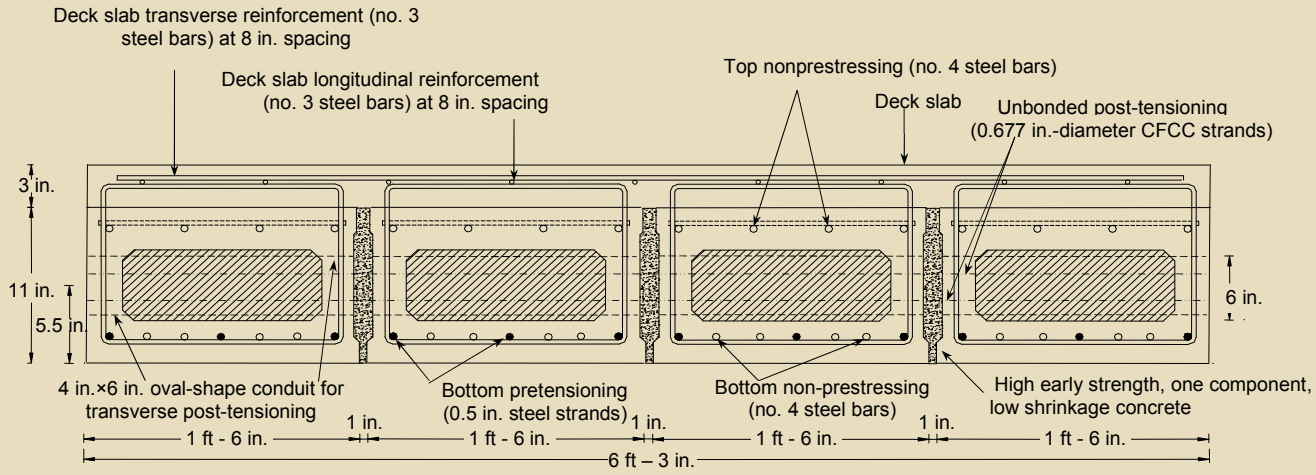

Figure 4. Cross-sectional details of conventional bridge model. Note: no. 3 = 10M; no. 4 = 13M; 1 in. = 25.4 mm; 1 ft = 0.305 m.

Table 1. Characteristics of prestressing, nonprestressing, and post-tensioning strands for CFCC bridge model

Characteristics	TPT CFCCs	Nonprestressing CFCCs	Prestressing CFCCs	CFCC stirrups
Grade	n.a.	n.a.	n.a.	n.a.
Nominal diameter, in.	0.67	0.60	0.60	0.355
Effective cross-sectional area, $in.^2$	0.23	0.179	0.179	0.09
Linear density, lb/in.	16.2	8.09	7.98	4.84
Minimum yield strength, ksi	n.a.	n.a.	n.a.	n.a.
Breaking load, kip	78.4	68.79	72	35.07
Tensile strength, ksi	336	371	392	365
Tensile modulus, ksi	22,335	22,770	22,625	24,075
Elongation at break, %	1.7	1.6	1.7	1.6

Source: Data from Tokyo Rope Mfg. Co. Ltd. 2007.
Note: CFCC = carbon-fiber-composite cable; n.a. = not applicable; TPT = transverse post-tensioning. 1 in. = 25.4 mm; 1 lb = 4.448 N; 1 kip = 4.448 kN; 1 ksi = 6.895 MPa.

Table 2. Characteristics of prestressing, nonprestressing, and post-tensioning strands for conventional bridge model

Characteristics	TPT CFCCs	Mild-steel reinforcing bars	Steel prestressing strands	Mild-steel reinforcing stirrups
Grade	n.a.	60	270	60
Nominal diameter, in.	0.67	0.5	0.5	0.375
Effective cross-sectional area, $in.^2$	0.23	0.2	0.153	0.11
Linear density, lb/in.	16.2	8.0	6.24	4.512
Minimum yield strength, ksi	n.a.	60	229.5	60
Breaking load, kip	78.4	18	41.3	9.9
Tensile strength, ksi	336	90	250	90
Tensile modulus, ksi	22,335	29,000	27,000	29,000
Elongation at break, %	1.7	9	1	9

Sources: Data from Hanson 2008; Soliman 2008.
Note: CFCC = carbon-fiber-composite cable; n.a. = not applicable; TPT = transverse post-tensioning. 1 in. = 25.4 mm; 1 lb = 4.448 N; 1 kip = 4.448 kN; 1 ksi = 6.895 MPa; Grade 60 = 410 MPa; Grade 270 = 1860 MPa.

beams were prestressed with an average force of 25 kip per strand.[10,11] Applying different levels of prestressing force for interior and exterior box beams simulated different cambers observed in the field. Elongations corresponding to the pretensioning forces were measured in both bridge models. **Tables 1** and **2** give the mechanical properties for the reinforcement used in the CFCC bridge model and conventional bridge model, respectively.

After prestressing the strands, concrete was placed in the formwork and vibrated using two pencil vibrators. In both cases the specified concrete compressive strength was 7000 psi (50 MPa), and the same concrete mixture proportions were approved for both models. However, the average compressive strength in the 28-day test of the exterior and interior box beams for the CFCC bridge model was 7630 psi (52.6 MPa). For the conventional bridge model, the recorded 28-day compressive strength of concrete was 6300 psi (43.0 MPa). The pretensioned forces were released after the concrete had attained a compressive strength of more than 5000 psi (34.0 MPa) to avoid possible cracking of the end blocks. The pretensioned strands were saw cut simultaneously from both ends of the box beams.

Figure 5. General view of precast, prestressed concrete carbon-fiber-composite cable bridge model.

Figure 6. General view of precast, prestressed concrete conventional bridge model.

Construction details of the bridge models

The precast concrete box beams were assembled adjacent to one another on 30-in.-high (760 mm) steel supports underneath the loading frame. After assembling the box beams on the supports, extruded polystyrene foam gaskets were attached at each end of the diaphragm to prevent leakage of grout into the ducts during the casting of the shear keys. The grouting of the shear keys was done with a high-early-strength, one-component, low-shrinkage concrete. After the shear key grout attained 7-day strength, an initial TPT force of 30 kip (130 kN) was applied at each diaphragm of both bridge models to prevent relative movement between the beams before casting the deck slab. The CFCC used for TPT in both bridge models was 0.7-in.-diameter (17 mm) cable made of seven primary strands. The deck slab of both bridge models was reinforced with transverse reinforcement spaced at 8 in. (200 mm) center to center and longitudinal reinforcement spaced at 6 in. (150 mm) center to center. In the CFCC bridge model, the longitudinal and transverse reinforcement consisted of 0.4-in.-diameter (10 mm) CFCC strands. Alternatively, the deck slab for the conventional bridge model was reinforced with no. 3 (10M) deformed mild steel reinforcing bars. A 3-in.-thick (75 mm) concrete deck slab with a compressive strength of 5000 psi (34.0 MPa) was cast. **Figures 5** and **6** show the completed CFCC bridge model and conventional bridge model ready for testing.

Test program

The bridge models were tested in two stages, simulating the conditions of highway bridges in service.

Stage 1: Uncracked deck slab

This stage resembled a newly constructed highway bridge with no longitudinal cracks. A strain-distribution test and a load-distribution test were conducted on the box-beam bridge models. In the strain-distribution test, the effects of different levels of TPT force and arrangement of TPT force on the distribution of transverse strains in the deck slab were investigated. The load-distribution test determined the load-deflection response of the bridge models across the width of the bridge for various levels and arrangement of TPT forces.

Stage 2: Cracked deck slab

This stage resembled a highway bridge with a partially cracked deck slab and cracked shear key due to service-load conditions. Three shallow longitudinal cracks of 0.25 in. (6.4 mm) in depth were cut at the shear-key locations using a circular diamond-blade saw. These shallow cracks directed the longitudinal cracks exactly at the shear-key locations. To simulate the longitudinal cracks, each individual box beam was subjected to a point load at the midspan and quarter-span locations. At the same time, the other three box beams were restrained from rotation using different support conditions at the midspan and quarter-span locations. A load-distribution test was then conducted on the cracked bridge model using different levels and arrangements of TPT forces.

Transverse strain-distribution test

The instrumentation was identical for both bridge models for the transverse strain-distribution test. To determine the transverse strains developed in the deck surface, a 30-deg skew grid of 27 strain gauges was placed transversely at shear-key locations (**Fig. 7**). The strain levels were monitored while applying different levels of TPT forces at different transverse diaphragm locations. Each diaphragm was subjected to three TPT forces: 20 kip, 40 kip, and 80 kip (89 kN, 180 kN, and 360 kN). Each of these forces was divided equally between the two unbonded CFCCs.

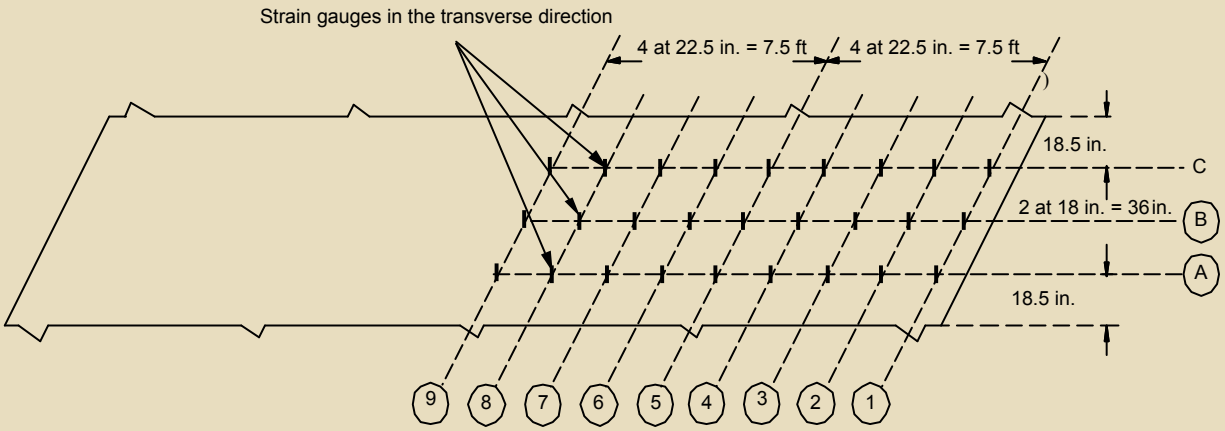

Figure 7. Shear-key locations and strain gauge layout on the deck slab for carbon-fiber-composite cable bridge model and conventional bridge model.
Note: 1 in. = 25.4 mm; 1 ft = 0.305 m.

The levels of the TPT forces varied, as did the number of diaphragms to which the forces were applied (five, four, or three). In the five-diaphragm case, the TPT forces were applied at all five diaphragm locations. In the four-diaphragm case, the TPT forces were applied to the end- and quarter-span diaphragms. In the three-diaphragm case, the TPT forces were applied at the end- and midspan diaphragm locations. The transverse strain-distribution test was conducted only in the uncracked stage.

Load-distribution test

Load-distribution tests were conducted to investigate the effect of the TPT force and the arrangements of different diaphragms on the behavior of bridge models across their widths. The cracking loads for both bridge models were computed using simple cracking moment and cracking load equations. The cracking load for the CFCC bridge model was 20 kip (89 kN), whereas for the conventional bridge model the cracking load (as determined by Hanson and Soliman)[10,11] was 16 kip (71 kN). Therefore, a load of 15 kip (80 kN) was selected for load distribution for both bridge models to avoid potential flexural cracking. This test was conducted for different magnitudes and arrangements of the TPT forces. The TPT forces were varied from 80 kip (360 kN) to 40 kip (180 kN) to 20 kip (89 kN) and then to 0 kip (0 kN). The magnitude of TPT forces varied with the number of diaphragms. The applied load was monitored with a load cell attached at the end of the actuator.

Linear motion transducers were attached at the midspan of each box beam to measure the corresponding deflections. The load-distribution test was conducted in both the uncracked and cracked stage of the bridge models. **Figure 8** shows a typical setup for the load-distribution test for CFCC and conventional bridge models with five diaphragms.

Ultimate load test

The purpose of the ultimate load test was to determine the ultimate flexural load–carrying capacity of the bridge models. In addition, the flexural responses of the unbonded TPT CFCC in the CFCC and conventional bridge models were evaluated. Both bridge models had a TPT force of 80 kip (360 kN) applied at all five diaphragms prior to the ultimate load test.

Different loading arrangements were used to load the bridge models during the ultimate load test. The CFCC bridge model was loaded uniformly at the midspan across its entire width using a steel spreader. The conventional bridge model was loaded eccentrically at the midspan of box beam B-2 using a steel spreader. Four linear motion transducers were attached at the midspan on both bridge models to monitor the deflections. Four strain gauges were attached to the deck surface at the midspan of each model to measure the concrete compressive strain. Center-hole load cells were attached at the dead end of the TPT strands to monitor the forces during the ultimate load test. To separate the elastic and inelastic energies, the bridge models were subjected to different loading and unloading cycles before the ultimate load test. **Figures 9** and **10** show the experimental setup and instrumentation for the ultimate load test of the CFCC and conventional bridge models, respectively.

Results and discussion

Strain-distribution test

Effect of magnitude of TPT force **Figure 11** presents the effect of the magnitude of the TPT force on the transverse strain values for the strain gauges located on shear key C-C in the CFCC and conventional bridge mod-

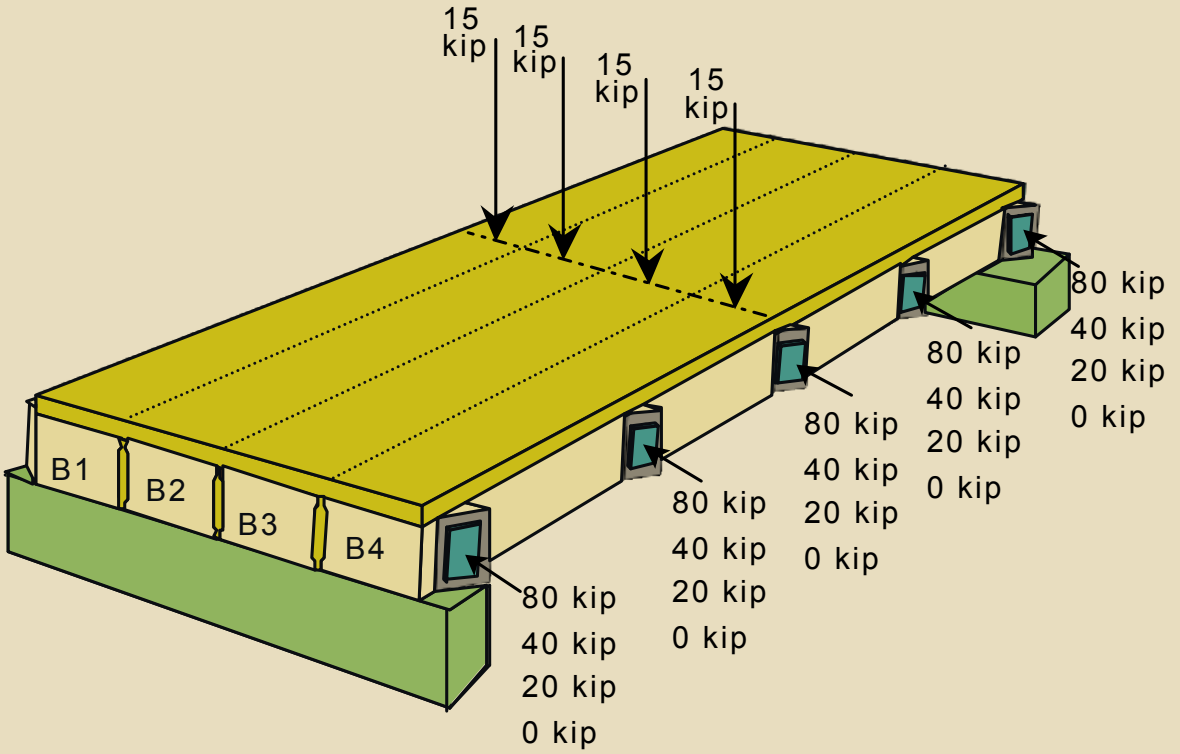

Figure 8. Load-distribution test with application of transverse post-tensioning forces at five diaphragms for the carbon-fiber-composite cable and conventional bridge models. Note: 1 kip = 4.448 kN.

els. Both bridge models experienced an increase in transverse strain with an increase in TPT force. For instance, point C-9 (Fig. 11), located at the midspan diaphragm of the CFCC bridge model, experienced transverse strains of -79 με, -153 με, and -204 με due to the application of 20 kip, 40 kip, and 80 kip (89 kN, 180 kN, and 360 kN), respectively, at the five diaphragms. In the conventional bridge model, the same point C-9 (Fig. 11) experienced transverse strains of -72 με, -143 με, and -212 με due to the application of 20 kip, 40 kip, and 80 kip, respectively, at the five

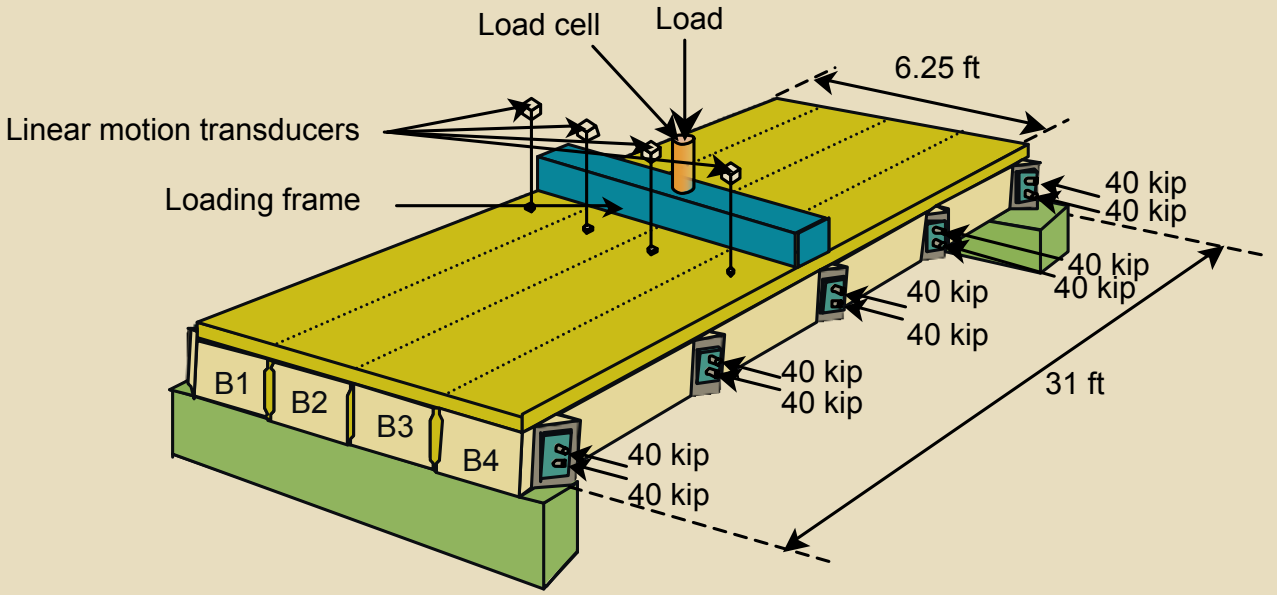

Figure 9. Experimental setup and instrumentation for ultimate load test of CFCC bridge model. Note: CFCC = carbon-fiber-composite cable. 1 ft = 0.305 m; 1 kip = 4.448 kN.

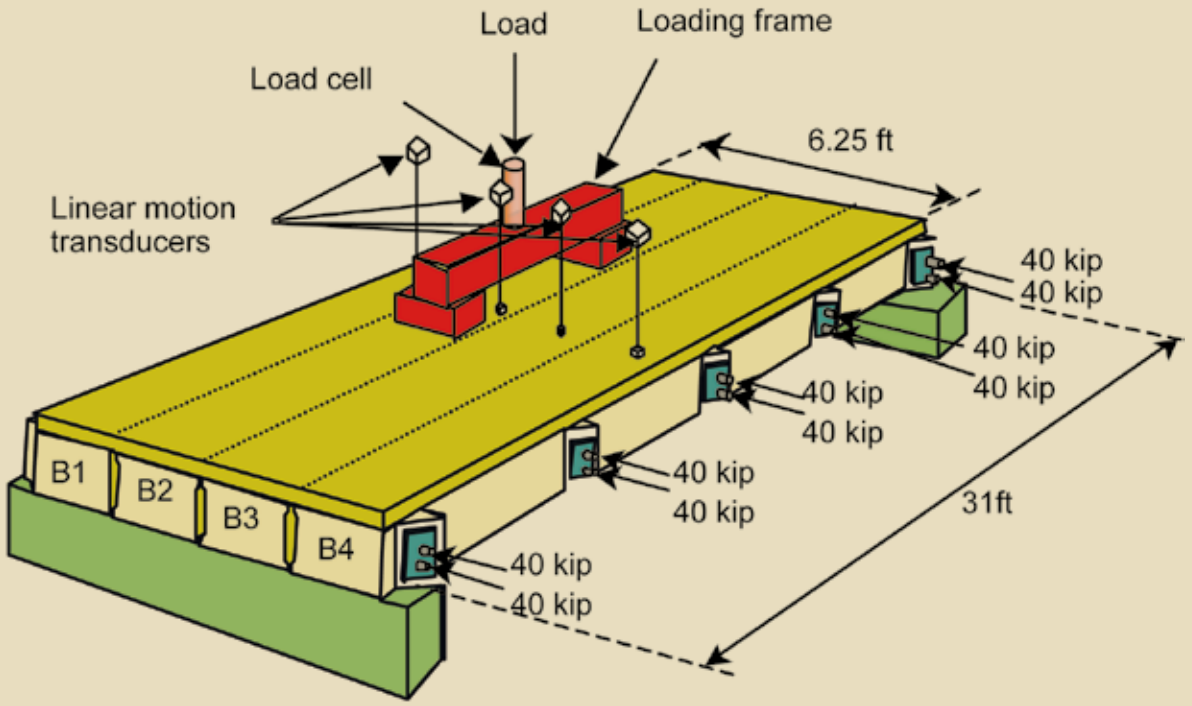

Figure 10. Experimental setup and instrumentation for ultimate load test of conventional bridge model. Note: 1 ft = 0.305 m; 1 kip = 4.448 kN.

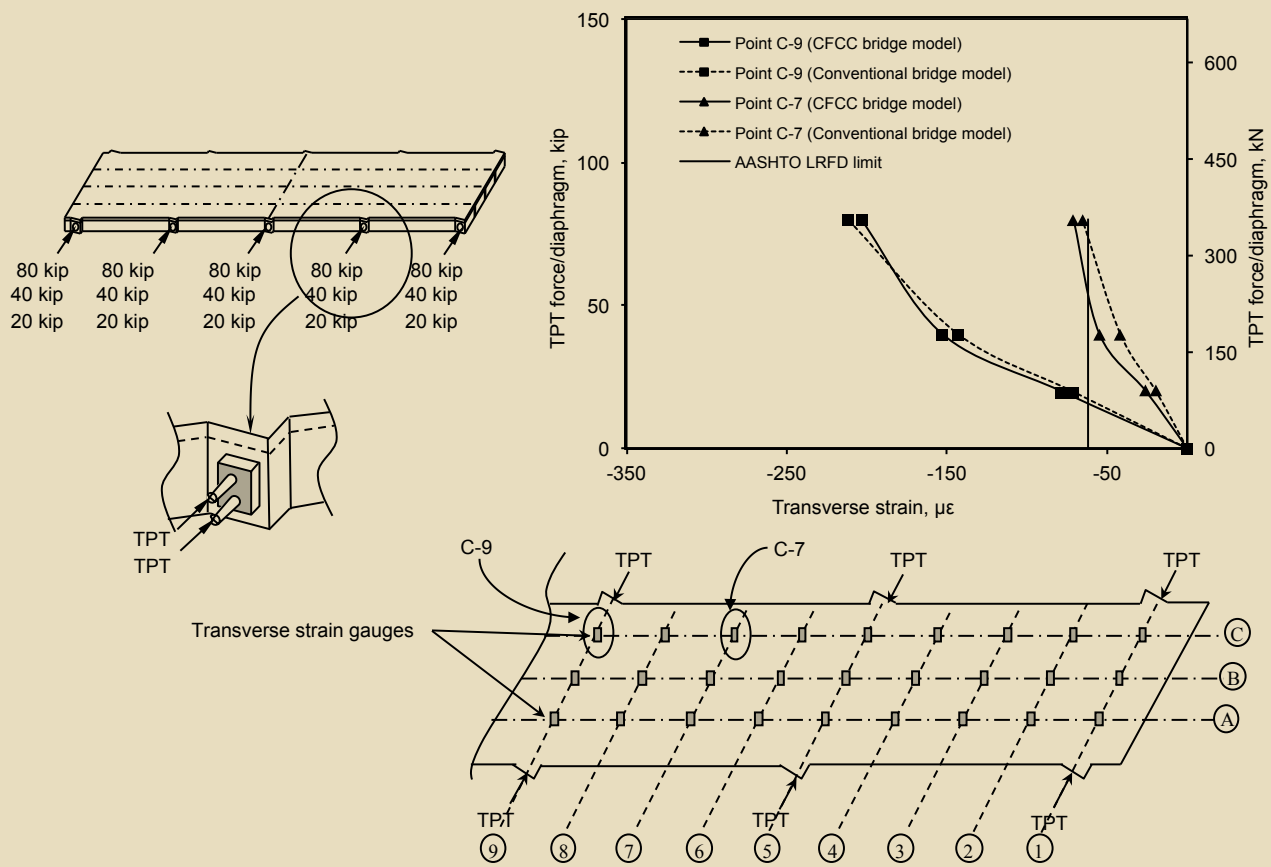

Figure 11. Transverse strains along shear key C-C for different TPT forces at five diaphragms for CFCC and conventional bridge models. Note: CFCC = carbon-fiber-composite cable; TPT = transverse post-tensioning. 1 kip = 4.448 kN.

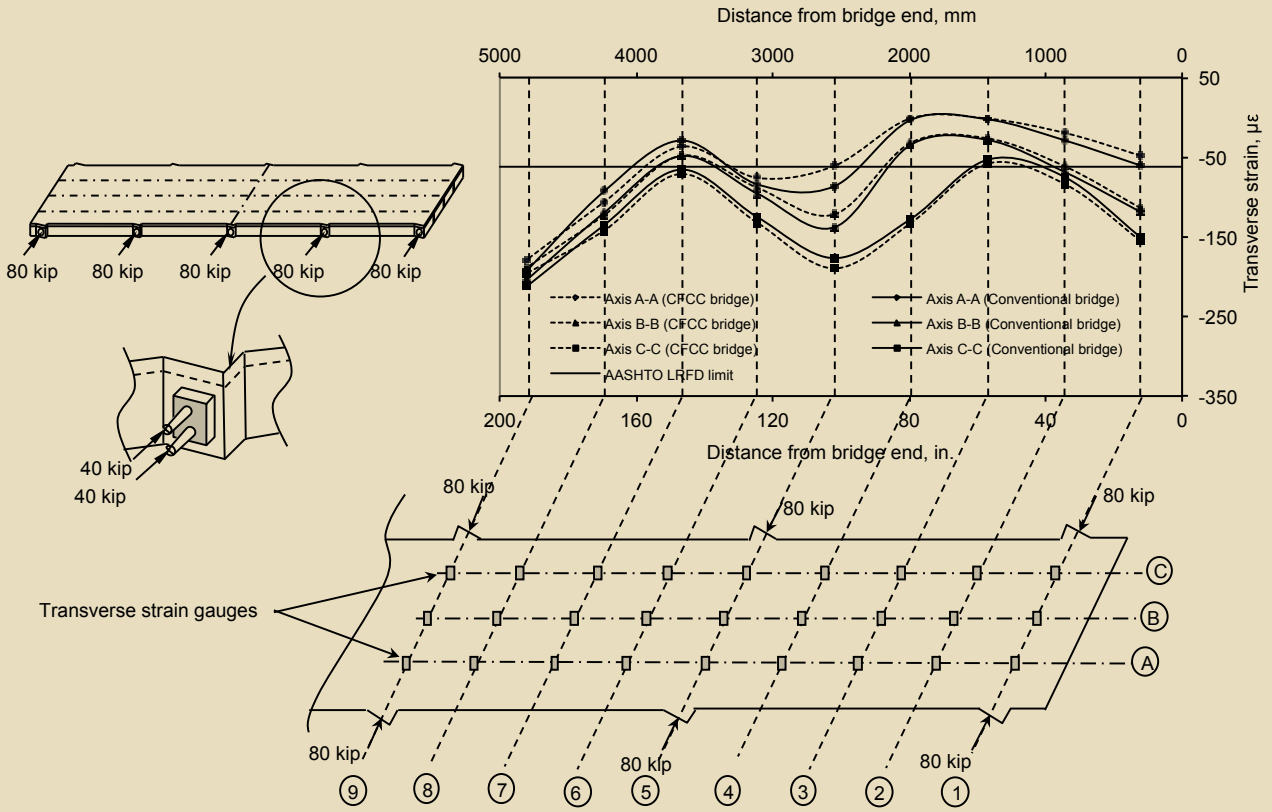

Figure 12. Transverse strains due to application of 80 kip at five diaphragms for CFCC and conventional bridge models. Note: CFCC = carbon-fiber-composite cable. 1 kip = 4.448 kN.

diaphragms.[10] Further, the increase in TPT force had an insignificant effect on the transverse strain located between the diaphragms. For instance, point C-7 (Fig. 11), located midway between the midspan diaphragm and quarter-span diaphragm of the CFCC bridge model, experienced transverse strains of -26 με, -55 με, and -71 με due to the application of 20 kip, 40 kip, and 80 kip, respectively, at the five diaphragms. In the case of the conventional bridge model, point C-7 (Fig. 11) experienced transverse strain values of -20 με, -42 με, and -66 με, respectively, for the same TPT force and diaphragm arrangement.[10] These results reflect an elastic behavior of the deck-slab concrete and suggest an identical behavior of both bridge models irrespective of the type of reinforcements used.

Effect of number of diaphragms The strain gauges located near the diaphragms experienced higher transverse strains. However, this effect was localized and the areas between the post-tensioned diaphragms experienced an insignificant level of strain due to TPT force, regardless of diaphragms.

In addition, the transverse strain decreased as the distance from the post-tensioned diaphragm increased. This phenomenon was observed in both CFCC and conventional bridge models. For example, when a TPT force of 80 kip (360 kN) was applied at five diaphragms of the CFCC bridge model, point B-9 (**Fig. 12**), located at the midspan diaphragm, experienced a transverse strain of -188 με. However, when a TPT force of 80 kip was applied at four diaphragms, the transverse strain at point B-9 was reduced to 0 με (**Fig. 13**). Similar behavior was observed in the case of the conventional bridge model, where point B-9 experienced a transverse strain of -204 με when a TPT force of 80 kip was applied at five diaphragms and a reduced strain level of -9 με when the same force was applied at four diaphragms of the conventional bridge model.[11] Figures 12 and 13 show the variation in transverse strain levels for the CFCC and conventional bridge models due to the application of a TPT force of 80 kip at five and four diaphragms, respectively.

The previous results show that the effect of the number of diaphragms on the transverse strains was similar in both bridge models and was independent of the type of reinforcement used.

Comparison with AASHTO recommendations A minimum transverse prestress of 0.25 ksi (1.7 MPa) due to TPT forces is recommended by the American Association of State Highway and Transportation Officials' *AASHTO LRFD Bridge Design Specifications, 3rd Edition—2005 Interim Revisions*[12] to make the box beams act as a single unit. However, it does not specify the contact

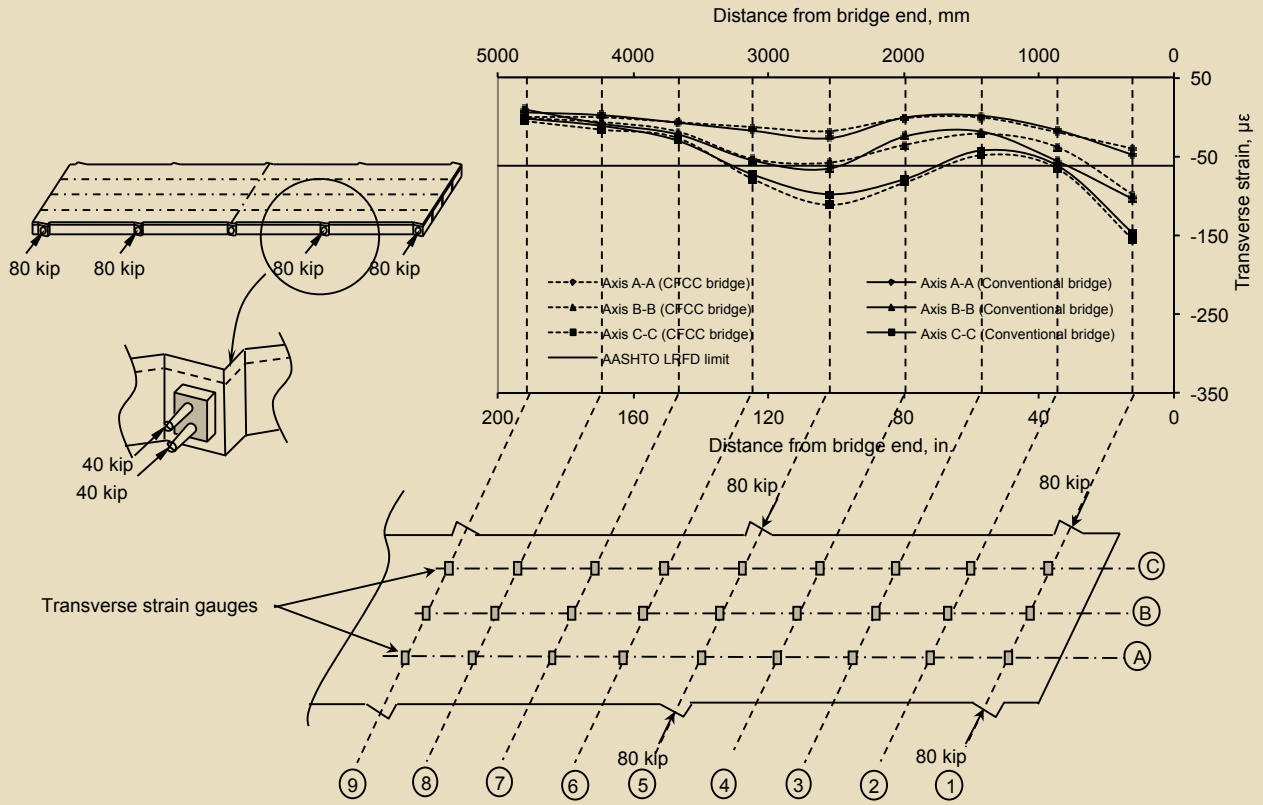

Figure 13. Transverse strains due to application of 80 kip at four diaphragms for CFCC and conventional bridge models. Note: CFCC = carbon-fiber-composite cable. 1 kip = 4.448 kN.

area over which this prestressing force should be introduced. In adjacent box-beam applications, it is not clear whether it should be the top shear-key area, the diaphragm-to-diaphragm contact area, or the full beam face.[13] Hence, the AASHTO LRFD specifications limit is converted to equivalent strain value (62 με)[10,11] to facilitate the comparison with the transverse strains experienced by the deck surface. From the transverse strain-distribution test for the CFCC bridge model and from the data presented in Fig. 12, a minimum of nine points experienced a transverse strain less than 62 με for all levels of TPT force and diaphragm arrangements. A minimum of eight points experienced strains less than the AASHTO LRFD specification limit for the conventional bridge model as depicted in Fig. 12. Most of the aforementioned points were located on shear key A-A (Fig. 12) and midway between the post-tensioned diaphragms. In addition, for a TPT force of 20 kip (89 kN), none of the strains complied with the AASHTO LRFD specifications limit in both bridge models. The strains experienced between the diaphragms did not meet the AASHTO LRFD specifications limit for various diaphragm arrangements. This may be attributed to the insignificant effect of TPT force in the region between the diaphragms.

Load-distribution test

Effect of magnitude of TPT force Both bridge models behaved similarly during the uncracked and cracked stages for different magnitudes of TPT force. In addition, in the uncracked stage the relative difference in the deflections between the adjacent box beams for both bridge models was insignificant. However, in the cracked stage, the loaded box beam always experienced the higher deflection, and the deflection decreased with increasing distance from the loaded box beam. This phenomenon was observed in both bridge models. For instance, when box beam B-3 (**Fig. 14**) of the CFCC bridge model was loaded in the uncracked stage, the relative differences in the deflections between box beams B-1 and B-3 (Fig. 14) were 0.01 in. (0.25 mm), 0.02 in. (0.5 mm), 0.02 in., and 0.03 in. (0.8 mm) for TPT forces of 80 kip, 40 kip, 20 kip, and 0 kip (360 kN, 180 kN, 89 kN, and 0 kN), respectively. The conventional bridge model had relative deflections of 0.02 in., 0.03 in., 0.03 in., and 0.04 in. (1 mm) for TPT forces of 80 kip, 40 kip, 20 kip, and 0 kip, respectively.[10] However, in the cracked stage the relative difference in the deflections between the box beams decreased with an increase in TPT force levels. For instance, the relative difference in the deflections between box beams B-1 and B-3 (Fig. 14) of the CFCC bridge model in the cracked stage were 0.02 in., 0.03 in., 0.05 in. (1.3 mm), and 0.08 in. (2 mm) for TPT forces of 80 kip,

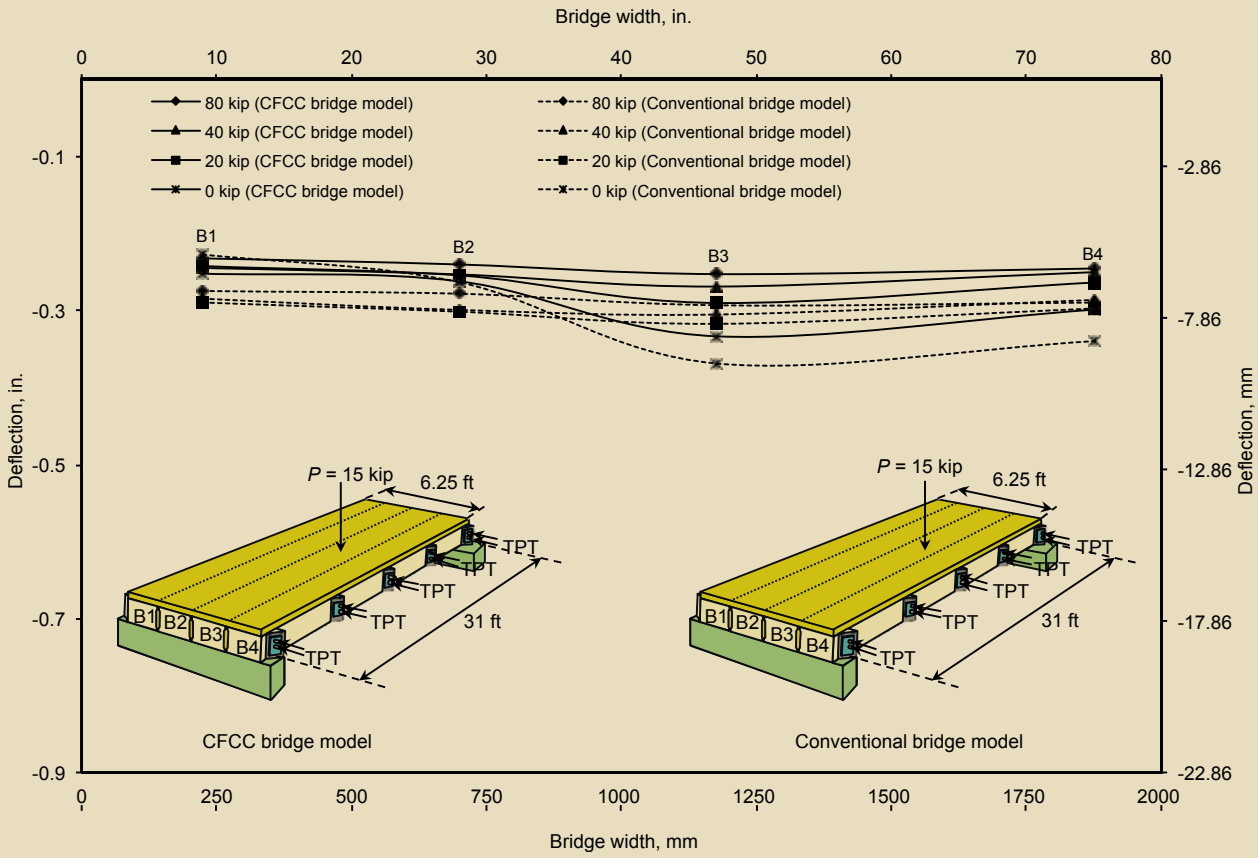

Figure 14. Effect of level of TPT forces at cracked stage for box beam B-3 for CFCC and conventional bridge models. Note: CFCC = carbon-fiber-composite cable; *P* = load; TPT = transverse post-tensioning. 1 ft = 0.305 m; 1 kip = 4.448 kN.

40 kip, 20 kip, and 0 kip, respectively. Figure 14 shows the effect of the level of TPT forces at a cracked stage for box beam B-3 for the CFCC and conventional bridge models. Similar observations were recorded for the conventional bridge model in the cracked stage. These results indicate that both bridge models behaved in a similar way and the type of reinforcement used had no effect on the load-distribution behavior.

Effect of number of diaphragms The number of diaphragms had an insignificant effect on the relative difference in deflections between the adjacent box beams in the uncracked stages of the CFCC and conventional bridge models. However, in the cracked stage the relative difference in deflections was lower in the case of three and five diaphragms compared with the four-diaphragm case. For instance, the relative differences in the deflections between box beams B-1 and B-3 (**Fig. 15**) of the CFCC bridge model in the cracked stage were 0.02 in. (0.5 mm), 0.04 in. (1 mm), and 0.03 in. (0.8 mm) due to the application of 80 kip (360 kN) at five, four, and three diaphragms, respectively.

When no TPT force was applied to any diaphragm, the relative difference in deflections between box beams B-1 and B-3 (Fig. 15) was 0.08 in. (2 mm). An identical case in the conventional bridge model recorded differential deflections of 0.03 in. (0.8 mm), 0.04 in. (1 mm), and 0.03 in. due to the application of 80 kip (360 kN) applied to five, four, and three diaphragms, respectively.[11] Alternatively, when the diaphragms were not subjected to the TPT forces, the observed relative deflection between B-1 and B-3 was 0.14 in. (3.5 mm). Figure 15 shows the effect of the number of diaphragms at the cracked stage for box beam B-3 due to application of an 80 kip TPT force for CFCC and conventional bridge models. These results indicate that the cases of five and three diaphragms had a greater influence on relative deflections compared with the four-diaphragm case in both bridge models. In addition, the observed results indicate an identical behavior of CFCC and conventional bridge models irrespective of the type of reinforcement used.

Ultimate load test

Load-deflection response **Figure 16** shows the ultimate load-deflection response for the CFCC and conventional bridge models. A TPT force of 80 kip (360 kN) was applied at all five diaphragms of both bridge models prior to the ultimate load test. Both bridge models were subjected to cyclic loading until the ultimate failure load was achieved.

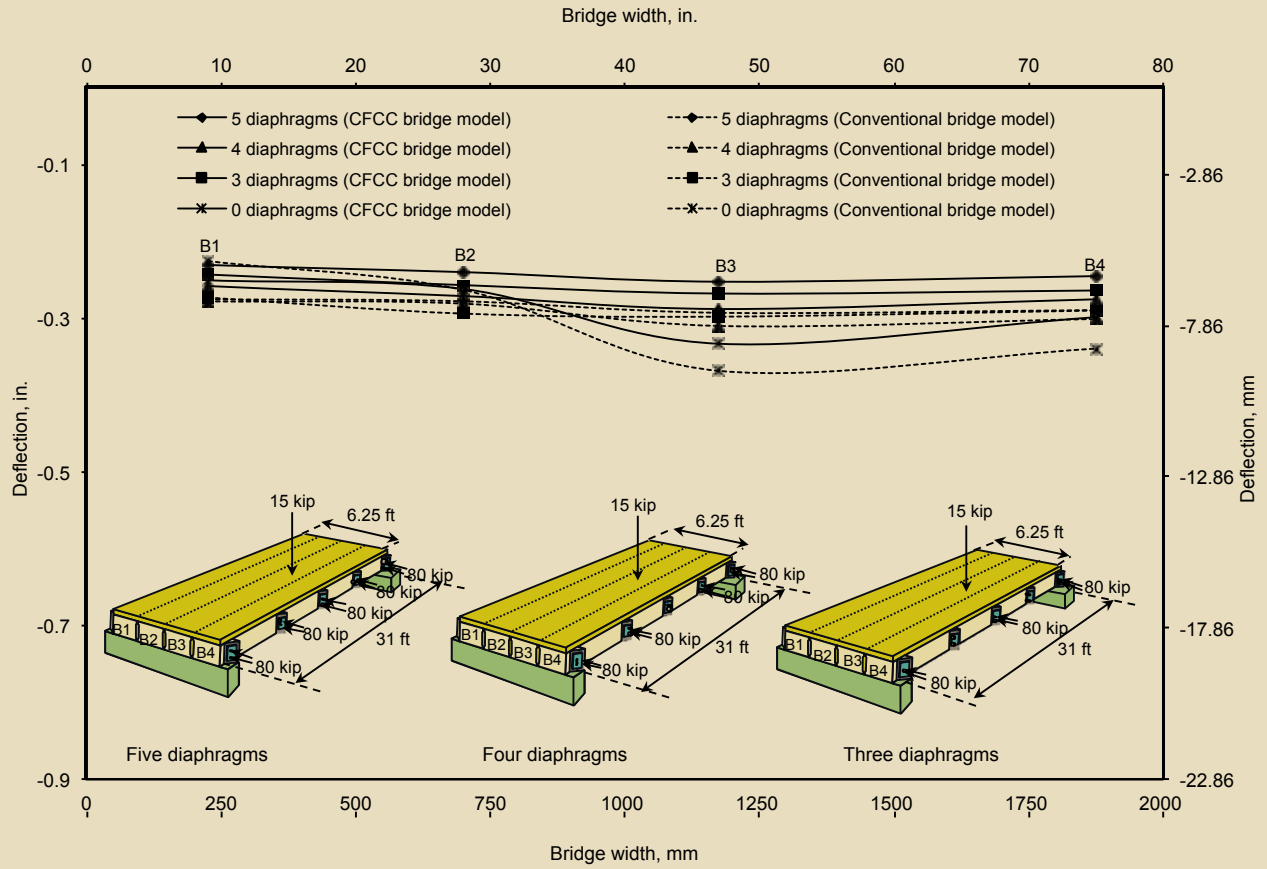

Figure 15. Effect of number of diaphragms at cracked stage for box beam B-3 due to application of 80 kip transverse post-tensioning force for CFCC and conventional bridge models. Note: CFCC = carbon-fiber-composite cable. 1 ft = 0.305 m; 1 kip = 4.448 kN.

Before the ultimate load cycle, the CFCC bridge model had achieved a cumulative residual deflection of 0.37 in. (9.4 mm), while the conventional bridge model recorded a cumulative deflection of 2.02 in. (51.3 mm).[10,11] The lower residual deflection of the CFCC bridge model was attributed to the brittle characteristics of the CFCC strands and the higher prestressing force. The conventional bridge model had a higher residual deflection due to the yielding of the steel strands and the lower prestressing force.

The load-deflection response for the CFCC bridge model was bilinear, with a change in slope at the cracking load of 20 kip (89 kN). The post-peak behavior of the load-deflection curve for the CFCC bridge model shows sudden failure due to crushing of concrete, as intended in ACI 440.[7] Alternatively, in the conventional bridge model a linear relationship was observed between the load and deflection up to 100 kip (445 kN).[10,11] Thereafter the deflection increased rapidly without any increase in load. This was attributed to the yielding of steel strands at 100 kip (445 kN). The ultimate load–carrying capacity for the CFCC bridge model was 120 kip (530 kN) with a corresponding deflection of 9.40 in. (239 mm). The maximum deflection after the complete failure of CFCC bridge model was 12.30 in. (312.4 mm). The observed ultimate load for the conventional bridge model was 104 kip (462 kN) with a corresponding deflection of 10.55 in. (268.0 mm). The maximum deflection observed for the conventional bridge model at ultimate failure was 24.17 in. (613.9 mm). That is, both bridge models exhibited sufficient deflection to provide warning of imminent failure. All beams deflected simultaneously during the ultimate load test for both bridge models.

Load–concrete strain response Readings obtained from the strain gauges at the midspans of both bridge models were used to plot the load–concrete strain response. **Figure 17** shows the compressive strain response of the deck-slab concrete with respect to the increase in load for the CFCC and conventional bridge models. Similar to the load-deflection response, the behavior of the deck-slab concrete in the CFCC bridge model was bilinear throughout the ultimate load test with a change in slope at the cracking load. On the other hand, the compressive strains in deck-slab concrete in the conventional bridge model increased proportionally with applied load up to 100 kip (445 kN), after which the compressive strains increased at a constant load, indicating yielding of steel reinforcement.[10,11] The CFCC bridge model exhibited a compressive failure with an ultimate compressive strain in concrete of

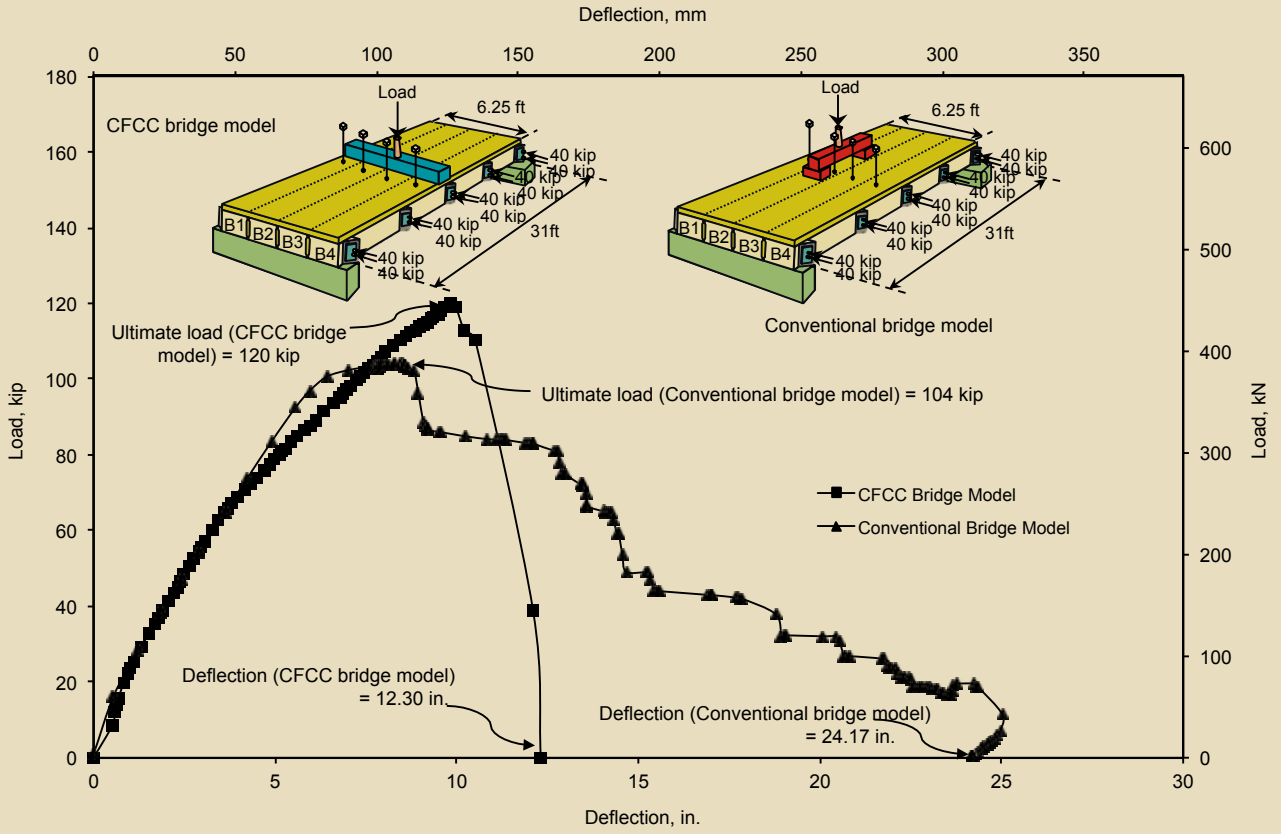

Figure 16. Ultimate load-deflection response of box beam B-2 for CFCC and conventional bridge models. Note: CFCC = carbon-fiber-composite cable. 1 in. = 25.4 mm; 1 ft = 0.305 m; 1 kip = 4.448 kN.

-2735 με, while the conventional bridge model exhibited a typical tensile failure with a compressive strain in the concrete of -1980 με.

Variation in TPT force The increase in the flexural stress of unbonded TPT strands mainly depends on the deformation of the entire model and is independent of the cross section of the member.[14] The dead end of each TPT strand had a center-hole load cell to monitor the variations in TPT forces during the ultimate load test. The unbonded TPT CFCCs remained intact during the entire ultimate load cycle and after the failure of both bridge models. In addition, the TPT CFCC strands in both bridge models showed an increase in TPT force during the load cycles due to the application of load and the deformation of the bridge model.

The strands at midspan exhibited the highest increase in TPT force, with the bottom strand having a higher force than the top strand. This phenomenon was observed in both bridge models. For instance, in the CFCC bridge model the bottom strand located at the midspan diaphragm experienced the highest increase in TPT force by 1.98 kip (8.81 kN), resulting in a total TPT force of 53.6% of the ultimate strength of the TPT CFCC as specified by the manufacturer. Similarly, in the conventional bridge model the bottom strand of the midspan diaphragm experienced the highest increase in TPT force by 2.3 kip (10 kN) and was stressed to 54% of the ultimate capacity specified by the manufacturer.[10, 11] These results suggest that both bridge models experienced a similar variation of TPT forces irrespective of the type of loading arrangement used.

Ductility The ductility of a bridge is its ability to sustain inelastic deformation while the load-carrying capacity is almost constant up to failure.[15] To allow for a comparison of bridge models designed in accordance with different design philosophies and subjected to different load configurations, an energy-based approach was adopted to evaluate their ductility. Both bridge models were subjected to various loading and unloading cycles before the ultimate load test to determine the ductility of the bridge model according to the energy ratio approach. Elastic and inelastic energies were then determined using the load-deflection response of the bridge model. The total energy was calculated by adding the elastic and inelastic energies. The energy ratio was then expressed as the ratio of inelastic energy absorbed to the total energy.[15] Bridges that have an energy ratio less than 69% exhibit a compressive failure, while those having an energy ratio greater than 75% exhibit a ductile failure.

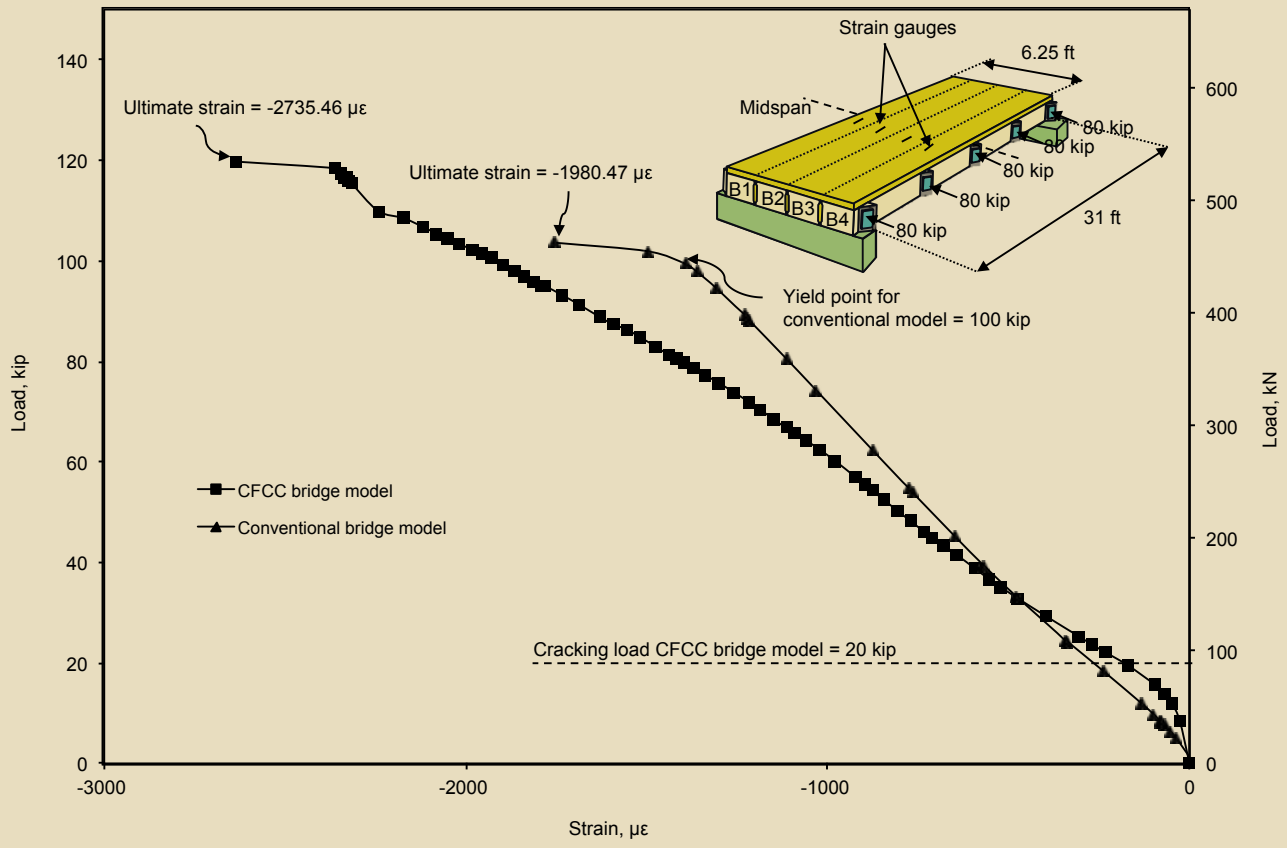

Figure 17. Ultimate load–concrete strain response for CFCC and conventional bridge models. Note: CFCC = carbon-fiber-composite cable. 1 ft = 0.305 m; 1 kip = 4.448 kN.

For the CFCC bridge model, the absorbed elastic, inelastic, and additional inelastic energies were 508 kip-in. (57,400 kN-mm), 232 kip-in. (26,200 kN-mm), and 196 kip-in. (22,100 kN-mm), respectively. The CFCC bridge model experienced a low energy ratio of 45.7% (**Fig. 18**) due to the lower residual deflections and additional inelastic energy absorbed. The lower residual deflections can be attributed to a lack of plastic behavior in the CFCCs.[15] In addition, the sudden compressive failure due to crushing of the concrete resulted in a low value of additional inelastic energy absorbed. For the conventional bridge model, the absorbed elastic, inelastic, and additional inelastic energies were 300 kip-in. (33,900 kN-mm), 549 kip-in. (62,000 kN-mm), and 738 kip-in. (83,400 kN-mm), respectively.[10,11] The conventional bridge model experienced a high energy ratio of 81.1%, thus exhibiting ductile failure (**Fig. 19**). As the failure of the conventional bridge model was initiated by yielding of the steel strands, the inelastic energy absorbed was higher, resulting in a higher energy ratio. However, the results do indicate the need to improve the ductility of the CFCC bridge model by exploring various design philosophies.

Failure mode As anticipated, flexural failure was observed for both bridge models. The CFCC bridge model was designed in accordance with ACI 440[7] as an over-reinforced section with a reinforcement ratio of 0.0055, which was greater than the balanced reinforcement ratio of 0.0021. The flexural compressive failure of the CFCC bridge model initiated due to crushing of concrete in the compression zone followed by the rupture of the top non-prestressed CFCCs (**Fig. 20**). The CFCC bridge model experienced the first flexural crack at a load of 20 kip (89 kN). New cracks were initiated and propagated between the quarter-span diaphragm and the midspan diaphragm when the bridge model was subjected to cyclic loading. Most of the cracks were concentrated in the midspan area, with a few cracks between the end-span and quarter-span diaphragms.

On the other hand, the conventional bridge model was designed in accordance with the MDOT design manual[4] as an under-reinforced section with a reinforcement ratio of 0.0017, which was lower than the balanced reinforcement ratio of 0.0023.[10, 11] The conventional bridge model experienced a typical ductile failure initiated due to yielding of the steel strands followed by crushing of the deck-slab concrete across the entire width of the bridge model. **Figure 21** shows the failure of the conventional bridge model. The first flexural crack was observed at the soffit of the box beam near the midspan region. New cracks initiated and propagated when the bridge model was subjected to

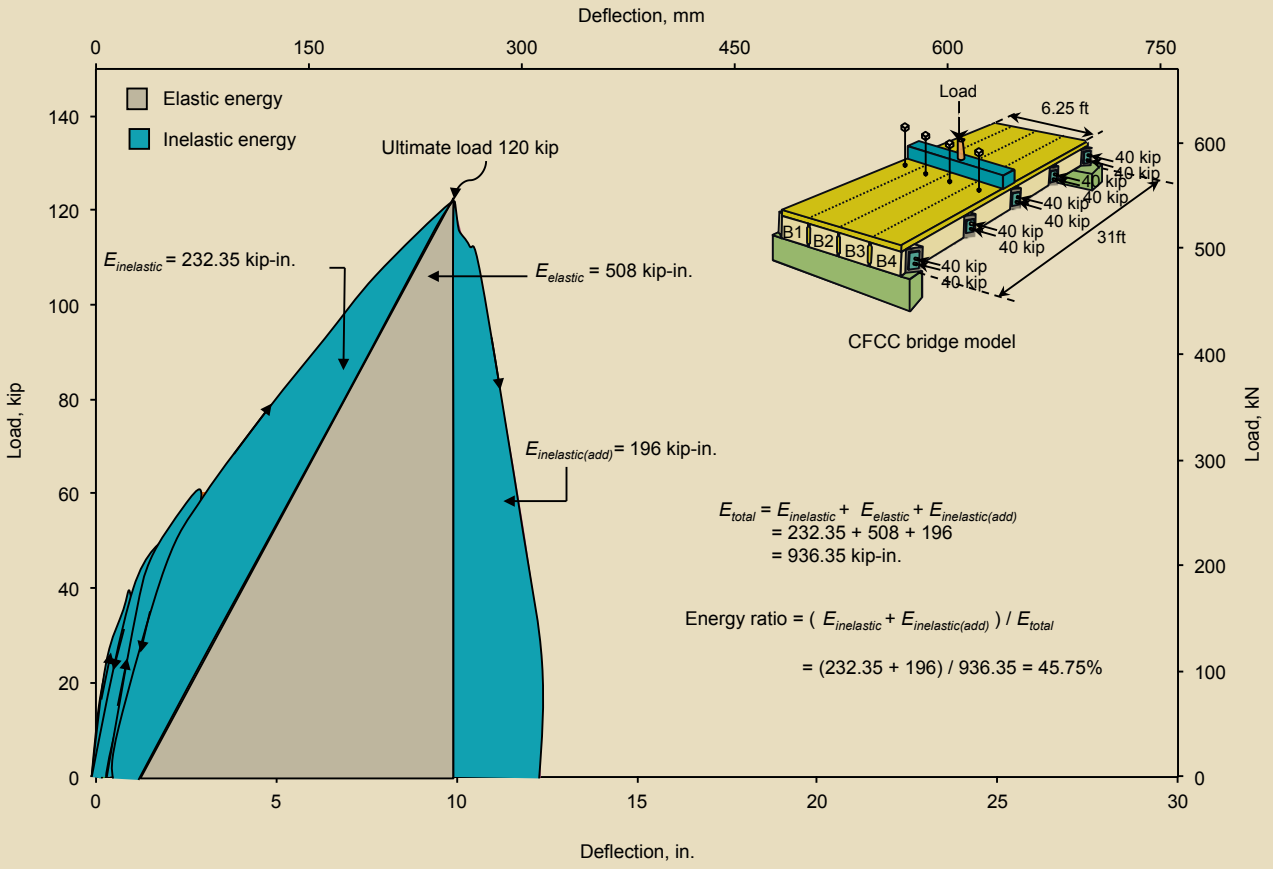

Figure 18. Energy ratio for CFCC bridge model. Note: CFCC = carbon-fiber-composite cable; $E_{elastic}$ = elastic energy absorbed by each bridge model; $E_{inelastic}$ = inelastic energy absorbed by each bridge model; $E_{inelastic(add)}$ = additional inelastic energy absorbed by the bridge model after the ultimate load; E_{total} = total energy absorbed by each bridge model. 1 in. = 25.4 mm; 1 ft = 0.305 m; 1 kip = 4.448 kN.

loading and unloading cycles. The propagation of cracks in each load cycle initiated the yielding of the bottom steel reinforcement, thus resulting in flexural ductile failure of the conventional bridge model. Both bridge models experienced the same deflection at their ultimate load carrying capacity. Both models experienced failure modes that were in close agreement with the theoretical analysis.

Conclusion

This research investigation compares the flexural performance of two box-beam bridge models reinforced and prestressed with CFCC and conventional steel strands. Both bridge models exhibited similar behavior irrespective of the type of reinforcements used. The following conclusions were drawn based on the results obtained from the experimental investigation:

- The results obtained from the strain-distribution and load-distribution tests conducted on the CFCC and conventional bridge models are in close agreement. This suggests that a bridge designed and constructed using CFCC materials responds to applied loads in the same way that a conventional bridge responds.
- The results obtained from the strain-distribution test of both bridge models indicate that the recommendation of 0.25 ksi (1.7 MPa) by AASHTO LRFD specifications as a minimum prestress cannot be met, especially between the diaphragm locations.
- The higher prestressing force and the brittle characteristics of CFCCs resulted in lower residual deflections for the CFCC bridge model. The lower prestressing force and the yielding properties of steel strands increased the residual deflections of the conventional bridge model. The CFCC bridge model and the conventional bridge model experienced cumulative residual deflections of 0.37 in. (9.4 mm) and 2.02 in. (51.3 mm), respectively, due to loading and unloading cycles.
- A similar variation in TPT force was observed in both bridge models, irrespective of the type of loading arrangement used, during the ultimate load test. The bottom cable of the CFCC bridge model was stressed to 53.6% of the ultimate capacity specified by the manufacturer, while that of the conventional bridge model was stressed to 54% of the ultimate capacity specified

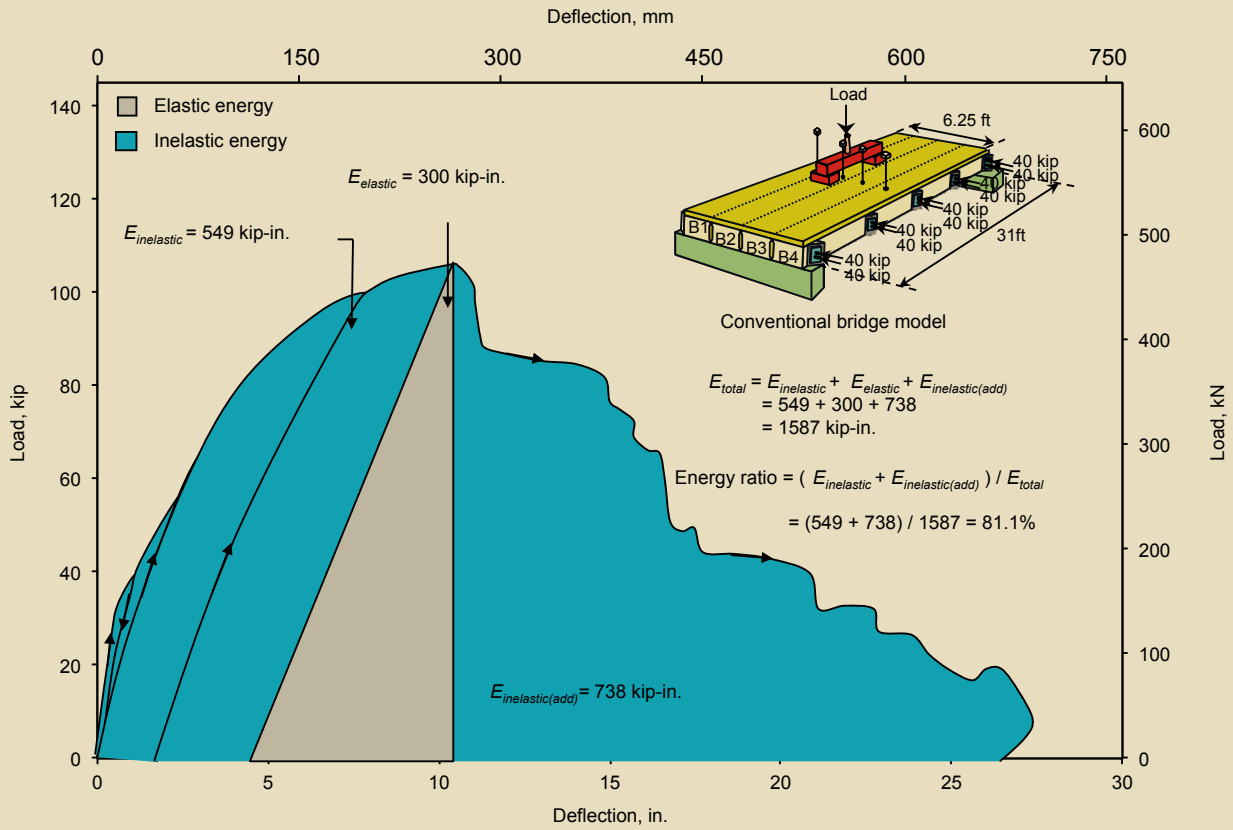

Figure 19. Energy ratio for conventional bridge model. Note: $E_{elastic}$ = elastic energy absorbed by each bridge model; $E_{inelastic}$ = inelastic energy absorbed by each bridge model; $E_{inelastic(add)}$ = additional inelastic energy absorbed by the bridge model after the ultimate load; E_{total} = total energy absorbed by each bridge model. 1 in. = 25.4 mm; 1 ft = 0.305 m; 1 kip = 4.448 kN.

by the manufacturer. Thus, the variation in TPT force was independent of the loading arrangement.

- All of the adjacent beams of both models deflected simultaneously with no differential deflections or rupture of the unbonded TPT CFCC strands. The unbonded transverse post-tensioning system is effective in distributing the load across the width of the bridge model.
- The CFCC bridge model had a compressive failure due to crushing of the concrete, while the conventional bridge model exhibited tensile failure due to yielding of the reinforcement. However, both bridge models

Figure 20. Failure of carbon-fiber-composite cable bridge model.

Figure 21. Failure of conventional bridge model.

experienced nearly the same deflection at ultimate load capacity.

- Members exhibiting compressive failure dissipate low inelastic energies, thus resulting in low energy ratios. The observed energy ratios for CFCC and conventional bridge models were 45.75% and 81.1%, respectively.

Acknowledgments

The United States Department of Transportation supported the experimental investigation presented in this paper through Contract No. DTOS59-06-G-00030 awarded to the Center of Innovative Materials Research at Lawrence Technological University in Southfield, Mich. The support of Brian Jacob of US-DOT and Louis Triansafilou of the Federal Highway Administration are appreciated. The support of Tokyo Rope Mfg. Co. Ltd. in Japan is acknowledged.

References

1. Structures Division. 1992. Modifications of the Current Shear Key and Tendon System for Adjacent Beam Prestressed Concrete Structures. Engineering Instruction EI 92-010, New York State Department of Transportation, Albany, NY

2. Needham, D. and D. Juntunen. 1997. Investigation of Condition of Prestressed Concrete Bridges in Michigan. Research and Technology Division. Michigan Department of Transportation (MDOT) Research report no. R-1348, Lansing, Mich. pp. 1–2.

3. Smith-Pardo, P., J. A. Ramirez, and R. W. Poston. 2006. Distribution of Compressive Stresses in Transversely Post-tensioned Concrete Bridge Decks. *ASCE Journal of Bridge Engineering*, V. 11, No. 1 (January–February): pp. 64–70.

4. MDOT. 2006. Prestressed Concrete Box-Beam and Post-tensioning Details. *MDOT Design Manual*. Lansing, Michigan: MDOT Bureau of Highway Development.

5. Bebawy, M. E. 2007. Optimum Transverse Post-tensioning Arrangement for Side-by-Side Boxbeam Bridges. M.Sc. thesis, Lawrence Technological University, Southfield, MI.

6. Abdelrahman, A. A., and S. H. Rizkalla. 1999. Deflection Control of Concrete Beams Pretensioned by CFRP Reinforcements. *ASCE Journal of Composites for Construction*, V. 3, No. 2 (May): pp. 55–62.

7. American Concrete Institute (ACI) Committee 440. 2006. *Guide for the Design and Construction of Structural Concrete Reinforced with FRP Bars (ACI 440.1R-06)*. Farmington Hills, MI: ACI.

8. Grace, N. F., T. Enomoto, S. Sachidananda, and S. Purvankara. 2006. Use of CFRP/CFCC Reinforcement in Prestressed Concrete Box-Beam Bridges. *ACI Structural Journal*, V. 103, No. 3 (January–February): pp. 123–131.

9. Grace, N. F., F. C. Navarre, R. B. Nacey, and W. Bonus. 2002. Design-Construction of Bridge Street Bridge—First CFRP Bridge in Unites States. *PCI Journal*, V. 47, No. 5 (September–October): pp. 20–35.

10. Hanson, J. Q. 2008. Effect of Level of Transverse Post-tensioning Forces on the Behavior of Side-by-Side Box-Beam Bridges Using Unbonded CFRP Strands. M.Sc. thesis, Lawrence Technological University, Southfield, MI.

11. Soliman, E. M. 2008. Effect of Number of Diaphragms on the Behavior of Side-by-Side Box-Beam Bridges Using Unbonded Transverse Post-tensioning CFRP Strands. M.Sc. thesis, Lawrence Technological University, Southfield, MI.

12. American Association of State Highway and Transportation Officials (AASHTO). 2005. *AASHTO LRFD Bridge Design Specifications, 3rd Edition—2005 Interim Revisions*. 3rd ed. Washington, DC: AASHTO.

13. El-Remaily, A., M. K. Tadros, T. Yamane, and G. Krause. 1996. Transverse Design of Adjacent Precast Prestressed Concrete Box Girder Bridges. *PCI Journal*, V. 41, No. 4 (July–August): pp. 96–113.

14. Grace, N. F., T. Enomoto, A. M. Ahmed, Y. Tokal, and S. Purvankara. 2008. Flexural Behavior of Precast Concrete Box Beams Post-tensioned with Unbonded, Carbon-Fiber-Composite Cables. *PCI Journal,* V. 60, No. 5 (July–August): pp. 62–82.

15. Grace, N. F., A. K. Soliman, G. Abdel-Sayed, and K. R. Saleh. 1998. Behavior and Ductility of Simple and Continuous FRP Reinforced Bars. *ASCE Journal of Composites for Construction*, V. 2, No. 4, (November): pp. 186–194.

Notation

$E_{elastic}$ = elastic energy absorbed by each bridge model

$E_{inelastic}$ = inelastic energy absorbed by each bridge model

$E_{inelastic(add)}$ = additional inelastic energy absorbed by the bridge model after the ultimate load

E_{total} = total energy absorbed by each bridge model

P = load

About the authors

Nabil F. Grace, PhD, P.E., is a University Distinguished Professor, dean of Engineering, and director of the Center for Innovative Materials Research for Lawrence Technological University in Southfield, Mich.

Kapil D. Patki, MSCE, is a research assistant for the Department of Civil Engineering at Lawrence Technological University.

Eslam M. Soliman, MSCE, is a research assistant for the Department of Civil Engineering at Lawrence Technological University.

Joseph Q. Hanson, MSCE, is a research assistant for the Department of Civil Engineering at Lawrence Technological University.

Synopsis

This paper compares box-beam bridge models reinforced and prestressed with different types of reinforcement.

The first box-beam bridge model was reinforced with prestressed carbon-fiber-composite cable (CFCC); the second box-beam bridge model was reinforced with conventional prestressed steel strands. The bridge models were identical in cross-sectional dimensions and were constructed by placing four box beams adjacent to one another and connected by means of transverse post-tensioning (TPT) forces at transverse diaphragms, shear keys, and deck slabs.

Load-distribution and strain-distribution tests were conducted on both bridge models in their uncracked and cracked stages. In addition, both bridge models were subjected to an ultimate load test to study the overall flexural response. The results show that the bridge models exhibited similar behavior during the strain- and load-distribution tests. As expected, the CFCC bridge model experienced a flexural compressive failure due to crushing of deck-slab concrete in the compressive zone, whereas the conventional bridge model experienced a flexural ductile failure due to yielding of steel strands. However, the CFCC bridge model exhibited a higher ultimate strength but a lower energy ratio compared with the conventional bridge model. In addition, the unbonded TPT strands of both bridge models remained intact, even after ultimate failure, and experienced a similar variation in TPT force during the ultimate load test. The results obtained from the strain distribution, load distribution, ultimate loads, modes of failure, deflection, strains, and energy ratios of CFCC and conventional bridge models are presented in this paper.

Keywords

Box beam, bridge, carbon-fiber-composite cable, CFCC, model, TPT, transverse post-tensioning.

Review policy

This paper was reviewed in accordance with the Precast/Prestressed Concrete Institute's peer-review process.

Reader comments

Please address any reader comments to journal@pci.org or Precast/Prestressed Concrete Institute, c/o *PCI Journal*, 200 W. Adams St., Suite 2100, Chicago, IL 60606.